Errors Due to the Reflectivity of Calibration Targets*

J. Randa, D.K. Walker, A.E. Cox, and R.L. Billinger
Electromagnetics Division
National Institute of Standards and Technology
Boulder, CO 80305, U.S.A.
randa@boulder.nist.gov

***Abstract*—For a microwave total-power radiometer, we consider the error introduced by neglecting the difference in the antenna reflection coefficient between when it views a distant scene and when it views a nearby calibration target. An approximate expression is presented for the error, and measurement results are presented that enable one to estimate the resulting uncertainty in the measured brightness temperature. This uncertainty ranges from about 0.1 K to several kelvins for the representative cases considered.**

Keywords-calibration, calibration target, microwave radiometer, radiometer, remote sensing, uncertainty analysis

I. INTRODUCTION

In microwave remote-sensing radiometry, calibration targets are often quite close to the sensing antenna, whereas the calibrated radiometer is used to measure very distant objects. This arrangement introduces two general types of errors for a total-power radiometer. One is that antenna-target interactions can affect the properties of the antenna such as its pattern and directivity, which may therefore be different when calibrating the radiometer than when viewing the earth. A second type of error is introduced by the change of the reflection coefficient at the antenna output (*i.e.*, at the reference plane between antenna and receiver) due to reflections from the calibration target that are not present when viewing a distant target. This difference in reflection coefficients results in different mismatch factors, and it also gives rise to changes in the system noise figure and available gain if the radiometer does not have an input isolator.

For an ideal blackbody calibration target both the target-proximity effects vanish, and for a very good target they are "very small." With modern microwave radiometers striving for ever smaller uncertainties, however, it becomes important to determine these effects. An uncertainty of 0.1 K or better, which some radiometers hope to achieve, is about 0.03 % of 290 K, and it is not immediately obvious that target proximity effects are negligible at that level. Here we consider the second type of error, that introduced by the difference in the antenna reflection coefficient when the antenna is pointed at a nearby calibration target as opposed to a very distant scene of interest.

In the next section, we summarize the approximate equations for the error introduced. In Section III we present measurement results, and Section IV contains estimates of the resulting uncertainties. Section V is devoted to a summary. A full account of this work can be found in [1].

II. CALCULATION

The reference plane of interest in this paper is the plane between the antenna and the rest of the radiometer, which we shall call plane 1. The spectral power delivered to the radiometer at plane 1 can be written as

$$p_1 = M_1 P_1 + p_{e,1}, \tag{1}$$

where p_1 is the spectral power delivered to the radiometer at plane 1, P_1 is the *available* spectral power at plane 1, $p_{e,1}$ is the effective delivered spectral power at the input plane 1 due to the radiometer's intrinsic noise, and M_1 is the mismatch factor at plane 1, given by

$$M_1 = \frac{\left(1-|\Gamma_{ant}|^2\right)\left(1-|\Gamma_r|^2\right)}{\left|1-\Gamma_{ant}\Gamma_r\right|^2}, \tag{2}$$

where Γ_{ant} and Γ_r are the reflection coefficients of the antenna and the radiometer, both at plane 1. In a measurement of brightness temperature, the radiometer views hot (h) and cold (c) calibration targets, as well as the unknown scene temperature (x), yielding three equations of the form of eq. (1). Assuming that M_1 and $p_{e,1}$ are the same for all three cases (h, c, and x), these three equations combine to yield the common form of the radiometer equation,

$$\left(T_x - T_c\right)_0 = \frac{(p_x - p_c)}{(p_h - p_c)}\left(T_h - T_c\right), \tag{3}$$

giving the temperature from the scene T_x in terms of the known brightness temperatures of the calibration targets (T_c and T_h) and the measured delivered spectral powers. The subscript 0 indicates that it is the result obtained with the assumption that M_1 and $p_{e,1}$ are the same for all three targets.

The point of this paper is that M_1 and $p_{e,1}$ are *not* the same for all three targets, and to estimate the error resulting from the use of eq. (3) in representative cases. The result for $(T_x - T_c)$, including the effect of differences in M_1 and $p_{e,1}$ for the three cases, can be written as [1]

$$T_x - T_c = \left(T_x - T_c\right)_0 (1+\delta_1) + \Delta_2 + \Delta_3. \tag{4}$$

The $(T_x - T_c)_0$ term is the answer that one would obtain using eq. (3). The δ_1 term is due to the different mismatch factors, and Δ_2 and Δ_3 result from the system's different available gain and noise temperature when the antenna reflection coefficient changes. Full expressions for δ_1, Δ_2,and Δ_3 are given in [1]. A useful approximate form can be obtained as follows. We assume that the antenna's reflection coefficient is the same when it is viewing the cold calibration target as when it is viewing the hot target. We use Γ_c to denote the antenna

reflection coefficient when it is viewing either calibration target, Γ_∞ for when the antenna is pointed at the distant scene, and Γ_r for the reflection coefficient of the radiometer at plane 1. We first assume that the effect is small, and so we keep only the lowest nonvanishing order in $\Delta\Gamma \equiv \Gamma_c - \Gamma_\infty$. We then also assume that each of the reflection coefficients Γ_c, Γ_∞, and Γ_r is small and save only terms to the lowest order in the reflection coefficients. With these approximations and some tedious algebra, the errors can be written as

$$\begin{aligned} \delta_1 &\approx 2\,\mathrm{Re}\left[(\Gamma_r - \Gamma_\infty)\Delta\Gamma\right], \\ \Delta_2 &\approx 2T_c\,\mathrm{Re}\left[(\Gamma_r - \Gamma_\infty)\Delta\Gamma\right] = \delta_1 T_c, \\ \Delta_3 &\approx 2X_1\,\mathrm{Re}\left(\Gamma_\infty \Delta\Gamma\right) + 2\,\mathrm{Re}\left(X_{12}\Delta\Gamma\right), \end{aligned} \tag{5}$$

where X_1 and X_{12} are noise parameters of the radiometer [2]. They are elements of the noise matrix, but referred to the input port. Thus they are related to the noise correlation matrix of Wedge and Rutledge [3] by $kX_1 = \overline{|c_1|^2}$, $kX_{12} = \overline{c_1 c_2^*}/S_{21}^*$, where k is Boltzmann's constant, the c's are wave amplitudes of the radiometer's intrinsic noise, and S_{21}^* is the complex conjugate of the 21 element of the scattering matrix.

Equation (5) gives the errors introduced by using the simplified radiometer equation, eq. (3). To estimate those errors, we need to know or estimate Γ_r, Γ_∞, $\Delta\Gamma$, X_1, and X_{12}. Γ_r can be measured by a vector network analyzer. In the next section we describe measurements of Γ_∞, $\Delta\Gamma$, and the noise parameters X_1 and X_{12}. We shall then return to obtaining actual numerical estimates of the errors in eq. (5).

III. Measurements

A. Setup

Measurements of Γ_c and Γ_∞ (and thus $\Delta\Gamma$) for several combinations of antenna and calibration target were performed in the NIST anechoic chamber. A vector network analyzer (VNA) was connected to the waveguide input of the antenna, and the antenna was mounted so that it pointed at the center of the target, which was mounted on a movable cart in the anechoic chamber. The absorber-covered platform runs on rails, and its position is computer controlled with a precision of 0.1 mm. The cart was stepped backward from the antenna, and the VNA measured the reflection coefficient of the antenna as a function of the distance from antenna to target. For each antenna, a measurement was also made with the target at the maximum distance allowed by the size of the anechoic chamber (about 4.5 m), to simulate viewing a distant scene. Measurements were made for several frequencies near 37 GHz and for several around 54 GHz, using several different combinations of antenna and target. For the sake of brevity, we present results for only two sets of measurements here. Other results can be found in [1].

The 37 GHz results that we present used an antenna and calibration target from the Airborne Imaging Microwave Radiometer (AIMR) [4]. This target is a commercially produced rectangular array of quadrahedral pyramids formed from a ferrous-loaded epoxy material molded on a bed of nails in an aluminum base. The array is covered with a styrofoam insulating layer and a mylar window roughly 0.25 mm thick. The overall transverse dimensions of the target are approximately 25 × 30 cm. The target was measured both with and without its cover; we will present the results with the cover in place since this corresponds to the configuration in which it is used. The antenna was a spare feed horn from AIMR. It consists of a Gaussian-optics lens antenna (GOLA), horn, dichroic plate, and grid polarizers. The half-power beam width at 37 GHz is 2.8°. The GOLA is mounted at the mouth of the feed horn and is constructed to reflect all energy below 30 GHz. The dichroic plate separates the beam into two frequencies, nominally 37 and 90 GHz, and the grid polarizers divide the beam into orthogonal polarizations, to yield four independent channels. In the actual AIMR instrument, the antenna system consists of the feed horn and an elliptical scan mirror, but in the present measurements only the conical horn was used. Measurements were made at 0.5 mm intervals from 34 cm to 35 cm, corresponding approximately to the horn-to-target distance in the actual AIMR instrument.

The second set of measurements we present was taken at 54 GHz. The target used will be referred to as the NASA target. It is a commercially produced circular disc approximately 33 cm in diameter, faced with an array of quadrahedral pyramids with an aspect ratio of 4:1. The base material of the target is aluminum, with pyramids formed by electrical discharge machining and coated with ferrous-loaded epoxy with a thickness of about 1 mm. It is intended for use at frequencies above about 35 GHz. The antenna used with this target was a commercially produced WR-19 cylindrical horn antenna with a dielectric lens and approximately 12.7 cm aperture, intended for use from 51 GHz to 56 GHz. At 53 GHz its 3-dB beamwidth is 3° in the H plane and 2.8° in the E plane. It will be called the NOAA antenna. The target was scanned over 10 mm, with measurements taken every 0.5 mm, starting from a minimum distance of about 2 cm between the antenna lens and the tips of the target.

B. Measurement Results

Fig. 1 plots the magnitude of the reflection coefficient Γ_c of the NOAA antenna when it views the NASA target, as a function of the cart position, at 54 GHz. It also shows the result for very large distance (4.5 m), Γ_∞. Fig. 1 clearly shows the effect of the target on the reflection coefficient of the antenna. Since the quantity of interest is actually $\Delta\Gamma = \Gamma_c - \Gamma_\infty$, we plot its magnitude in Fig. 2. We see that the magnitude of $\Delta\Gamma$ ranges from about 0.0005 to about 0.0035.

Results for $|\Delta\Gamma|$ for the AIMR antenna viewing the AIMR target are shown in Fig. 3 for a scan from 34 to 35 cm, the approximate distance between the AIMR antenna aperture and the target in the actual radiometer. The reflection coefficient of the AIMR antenna itself (distant target) is about 0.075, considerably larger than that for the NOAA antenna at 54 GHz (0.031). Also, $|\Delta\Gamma|$ is considerably larger (~0.12 maximum)

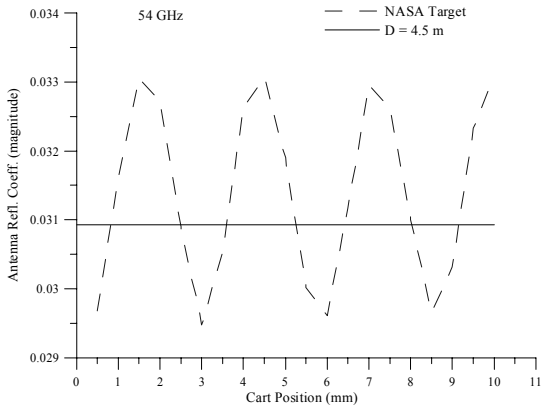

Fig.1 Measured reflection coefficient of antenna as function of cart position.

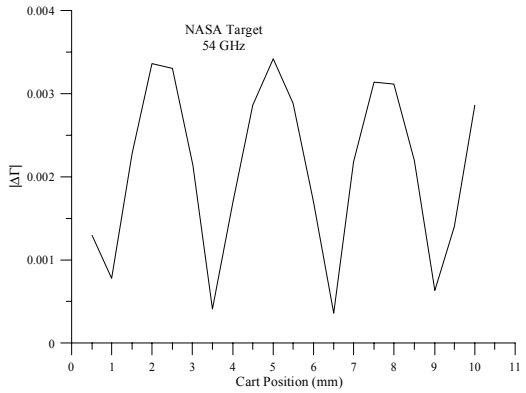

Fig. 2 Magnitude of $\Delta\Gamma$ for NASA target as function of cart position.

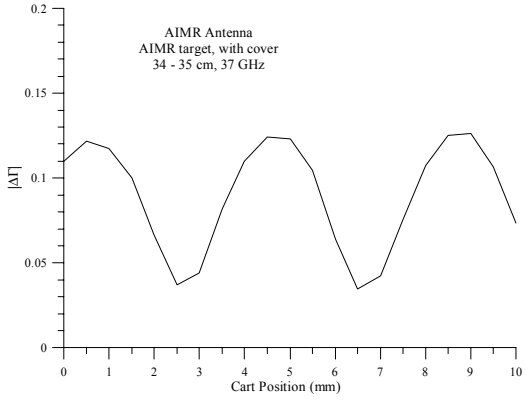

Fig. 3 $|\Delta\Gamma|$ for AIMR antenna and AIMR target.

for the AIMR antenna-target combination, which will in turn lead to larger errors from its neglect.

C. *Values of Noise Parameters*

In order to estimate the error incurred by using eq. (3), we also need to measure or estimate the noise parameters X_1 and X_{12} of the radiometer. To obtain realistic values for our estimates, we measured the noise parameters of the AIMR radiometer at 37 GHz, using a method similar to that of Meys [5] with the results that $X_1 \approx 223$ K and $|X_{12}| \approx 37.6$ K.

Another convenient case to consider is a total-power radiometer with an isolator on the input. In that case, X_1 and X_{12} can be calculated; they are given by

$$X_1 \approx T_I, \quad X_{12} \approx -T_I S_{11}^I, \tag{6}$$

where I refers to the isolator, and we have assumed $|S_{11}{}^I|$, $|S_{22}{}^I|$, and $|S_{21}{}^I|$ are all small. Note that in this case $\Gamma_r \approx S_{11}^I$, and eq. (6) leads to $\Delta_2 + \Delta_3 = 0$, so that the only remaining error is δ_1, which is due to the different mismatch factors. Representative numerical values are given below.

IV. Numerical Estimates

We can now estimate the magnitude of the error introduced by using the simple form of the radiometer equation, eq. (3). From eqs. (4) and (5), we see that the total error depends on the value of Γ_r. The value of Γ_r will obviously vary from one radiometer to another, but it will typically be small. If we set $\Gamma_r = 0$, it will have little effect on the numerical results and no effect on the qualitative conclusions. We therefore do so and refer to the resulting error and uncertainty as $\Delta^{(0)}$ and $u^{(0)}$. With $\Gamma_r = 0$, the total error takes the form

$$\Delta_{tot}^{(0)} \approx 2(X_1 - T_{x,0})\,\mathrm{Re}(\Gamma_\infty \Delta\Gamma) + 2\,\mathrm{Re}(X_{12}\Delta\Gamma), \tag{7}$$

where $T_{x,0} = (T_x - T_a)_0 + T_a$. In evaluating the error and uncertainty for an actual radiometer, one would proceed as below but use the actual value of $(\Gamma_r - \Gamma_\infty)$ rather than Γ_∞ in the first term of eq. (7).

We work in terms of the standard uncertainties u [6]. These are estimates of the root-mean-square (RMS) values of the errors, where the mean is taken over reasonably probable measurement possibilities, which in this case means over reasonable values of the unknown parameters. Thus

$$\begin{aligned} u_{tot}^{(0)} &= \sqrt{\left\langle \left(\Delta_{tot}^{(0)}\right)^2 \right\rangle} \\ &= 2\left\{ (X_1 - T_{x,0})^2 \left\langle (\mathrm{Re}(\Gamma_\infty \Delta\Gamma))^2 \right\rangle + \frac{1}{2}|X_{12}|^2 \left\langle |\Delta\Gamma|^2 \right\rangle \right\}^{1/2} \end{aligned} \tag{8}$$

where we have averaged over the (unknown) phase between X_{12} and $\Delta\Gamma$, which introduces the factor of ½ in the second term. The remaining averages are over the distance between antenna and calibration target. They can be evaluated from our measured results.

We will treat two specific cases as a demonstration and to obtain representative results. General features will be discussed in Section V. The first case is that of the AIMR antenna with the AIMR target at the approximate operating distance in the radiometer, 34 – 35 cm. From our measurements, X_1 = 223 K, $|X_{12}|$ = 37.6 K, $\left\langle (\mathrm{Re}(\Gamma_\infty \Delta\Gamma))^2 \right\rangle = 3.25\times10^{-5}$, $\left\langle |\Delta\Gamma|^2 \right\rangle = 0.00957 = |\Delta\Gamma|_{RMS}{}^2$. Consequently, for values of $T_{x,0}$ in the range of 200 K – 300 K,

$$u_{tot}^{(0)} \approx \sqrt{2}\,|X_{12}|\,|\Delta\Gamma|_{RMS} \approx 5.2\,K\,. \qquad (9)$$

This is somewhat larger than would be expected from the checks comparing different calibration methods for this instrument [7], which indicated agreement to within about 2 K. There are several possible explanations for this apparent discrepancy. The measurement of the AIMR noise parameters took much longer than the time over which the instrument is designed to be stable, and therefore the measured value of $|X_{12}|$ may be an overestimate. Also, only the feed horn (without the reflector) of the AIMR radiometer was used in these tests, and it was a spare, which may not be identical to the one in the actual radiometer. Finally, it should be borne in mind that the result for the standard uncertainty in eq. (9) is an RMS value, with the average taken over a range of antenna-to-target distances, whereas the actual AIMR instrument corresponds to just one of those distances, which could well be a relatively fortunate one. In particular, eq. (8) entailed an average of $[\mathrm{Re}(X_{12}\Delta\Gamma)]^2$ over the relative phase between X_{12} and $\Delta\Gamma$. If X_{12} and $\Delta\Gamma$ happen to be out of phase for AIMR, this dominant contribution to the error vanishes, and the remaining error is less than 1 K. (The distinction between "error" and "uncertainty" is important here—and elsewhere. The error is the difference between the value obtained and the true value. The uncertainty represents an RMS average expected value of the error.)

If the radiometer had an isolator on the front end, then one would have $X_1 \approx T_a$, $X_{12} \approx -T_a S_{11}^I$, and the uncertainty can be substantially reduced provided $|S_{11}|$ of the isolator is small. If $|S_{11}| = 0.025$, then for $T_{x,0} - T_a$ less than about 50 K, $u_{tot}^{(0)} \approx 1$ K.

The second case we consider is the NOAA antenna with the NASA target at 54 GHz and a separation distance of about 2 – 3 cm. For this combination of antenna and target, $\left\langle (\mathrm{Re}(\Gamma_\infty \Delta\Gamma))^2 \right\rangle = 2.2\times10^{-9}$ and $|\Delta\Gamma|_{RMS}^{\ 2} = 5.4\times10^{-6}$. The first term in eq. (8) is therefore almost always negligible, and $u_{tot}^{(0)} \approx 0.0033\,|X_{12}|$. The value of $|X_{12}|$ depends on the specific radiometer. Since $|X_{12}|$ could be of the order of 100 K or more, particularly at high frequencies, $u_{tot}^{(0)}$ may well be several tenths of a kelvin. This is likely to be significant for many radiometers that are to be deployed in the next decade. If the radiometer has a front-end isolator, $u_{tot}^{(0)} \approx 0.95\ K \times |S_{11}^I|$, and the uncertainty can be brought under 0.1 K for this combination of antenna and target.

V. Summary

We have considered the error arising from the difference in antenna reflection coefficient when viewing a distant scene and a nearby calibration target, and using the common, simple form for the radiometer equation of a total power radiometer, eq. (3). An expression was derived for the approximate error, and measurements were performed that enabled us to estimate the resulting standard uncertainty for some representative cases. For radiometers without front-end isolators, the uncertainty can be as large as several kelvins, depending on the particular antenna, target, and receiver. Even in relatively good cases the uncertainty can be a few tenths of a kelvin. Use of a well-matched isolator reduces the error significantly. The magnitudes of the antenna and receiver reflection coefficients and the target reflectivity are critical factors in determining the size of the error. For an unisolated radiometer, the receiver noise parameters are also important. Because of the variation of the effect with the distance between antenna and target, the situation in an actual case could be significantly better or worse than our estimates, which were RMS results for a range of distances and relative phases.

Our results suggest that for radiometers employing a calibration target close to the antenna, the effects of $\Delta\Gamma \neq 0$ need to be considered if uncertainties are to be of the order of a few kelvins or less. In that case, $\Delta\Gamma$ and Γ_∞ should be measured; Γ_r, X_1, and X_{12} should be measured or estimated; and the uncertainties should be estimated. In fact, if everything is measured, one can use the full radiometer equation to explicitly correct for $\Delta\Gamma$ and not worry about introducing errors by neglecting δ_1, Δ_2, and Δ_3. Our treatment assumed two nearby calibration targets and a distant scene. We expect an analogous effect when one of the calibration targets is nearby and the other is distant, such as cold space.

Acknowledgments

We thank Al Gasiewski and Vladimir Leuski of the NOAA Environmental Technology Laboratory for loan of an antenna and for helpful discussions, Paul Racette and Jeff Piepmeier of NASA Goddard Space Flight Center for loan of a target and for helpful discussions, and Dennis Camell of NIST for assistance in using the NIST anechoic chamber. We thank the Meteorological Service of Canada, Environment Canada (Atmospheric and Climate Science Directorate and Canadian Ice Service) for the use of the AIMR system.

References

[1] J. Randa, D.K. Walker, A.E. Cox, and R.L. Billinger, "Errors resulting from the reflectivity of calibration targets," IEEE Trans. Geoscience and Rem. Sens., in press.

[2] J. Randa, "Noise-parameter uncertainties: a Monte Carlo simulation," *J. Res. NIST*, vol. 107, pp. 431 – 444, Sept./Oct. 2002.

[3] S.W. Wedge and D.B. Rutledge, "Wave techniques for noise modeling and measurement," *IEEE Trans. Microwave Theory Tech.*, vol. 40, pp. 2004 – 2012, Nov. 1992.

[4] M.J. Collins, F.G. Ross Warren, and J. Lawrence Paul, "The Airborne Imaging Microwave Radiometer-Part I: Radiometric Analysis," *IEEE Trans. Geoscience and Remote Sensing*, vol. 34, pp. 643-655, March1996.

[5] R.P. Meys, "A wave approach to the noise properties of linear microwave devices," *IEEE Trans. Microwave Theory Tech.*, vol. MTT-26, pp. 34 – 37, Jan. 1978.

[6] "ISO Guide to the Expression of Uncertainty in Measurement", Int. Org. Standard., Geneva, Switzerland, 1993.

[7] J. Haggerty, A. Cox, and C. Walther, "Extending the Calibration Range for the Airborne Imaging Microwave Radiometer (AIMR) Part II: Using the Sky for Low Temperature Calibration Points," presented at the First International Microwave Radiometer Calibration Workshop, College Park, Maryland, October 30-31, 2000.

IGARSS 2004 Conference Digest
Paper 4TH_70_02

2004 IEEE International Geoscience and Remote Sensing Symposium
20 – 24 September, 2004
Anchorage, Alaska